G. Saibene, P. J. Lomas, M. Becoulet, R. Sartori, A. Loarte, R. Budny, V. Parail,
K. D. Zastrow , M. von Hellermann, M. Beurskens, Y. Andrew, A. Kallenbach,
P. Hennequin, W. Suttrop, J. Stober, S. Sharapov, M. Zerbini
and JET EFDA Contributors

The Effect of Plasma Shape on Density and Confinement of ELMy H-Modes in JET

The Effect of Plasma Shape on Density and Confinement of ELMy H-Modes in JET

G. Saibene[1], P. J. Lomas[2], M. Becoulet[3], R. Sartori[1], A. Loarte[1], R. Budny[4],
V. Parail[2], K. D. Zastrow[2], M. von Hellermann[5], M. Beurskens[5], Y. Andrew[2],
A. Kallenbach[6], P. Hennequin[7], W. Suttrop[6], J. Stober[6], S. Sharapov[2], M. Zerbini[8]
and JET EFDA Contributors*

[1]*EFDA Close Support Unit, Garching, MPI fur Plasmaphysik, 2 Boltzmannstrasse, Garching, Germany*
[2]*Euratom/UKAEA Association, Culham Science Centre, Abingdon, OX14 3EA, UK*
[3]*Association Euratom-CEA, Cadarache, F-13108 St. Paul-lez-Durance, France*
[4]*PPPL Princeton University, P.O Box 451, Princeton, NJ 08543, USA*
[5]*FOM/Euratom instituut v plasmafysica 'Rijnhuizen', Nieuwegein, Trilateral Euregio Cluster, The Netherlands*
[6]*Association Euratom-IPP, MPI fur Plasmaphysik, 2 Boltzmannstrasse, Garching, Germany*
[7]*Laboratoire PMI, Ecole Polytechnique, 91128 Palaiseau, France*
[8]*Associazione Euratom-ENEA, V E Fermi 47, 00044 Frascati, Italy*
* See the appendix of JET EFDA contributors (prepared by J. Paméla and E.R Solano),
*See appendix of the paper by J.Pamela "Overview of recent JET results",
Proceedings of the IAEA conference on Fusion Energy, Sorrento 2000

ABSTRACT

This paper presents the results of experiments carried out in JET to investigate the confinement properties of NB heated high density ELMy H-modes, focusing on the effects of plasma triangularity δ on the relationship between energy confinement and density.

1. GLOBAL PERFORMANCE OF HIGH D PLASMAS.

Previous experiments in JET [1] and other divertor tokamaks have shown that the thermal energy confinement time and the maximum density achievable in steady state for a given confinement enhancement factor increase with δ. Recent experiments in JET have confirmed and extended these earlier results, up to a plasma triangularity of $\delta\sim0.5$ ($\kappa\sim1.75$), achieving a line average density $n_e\sim1.1n_{GR}$ and $H_{97}\sim0.85$ (Fig.1). In this plasma configuration, at 2.5MA/2.7T ($q_{95}\sim3$), a line average density $\sim90\%$ n_{GR} with $H_{97}=1$ and $\delta_N\sim2$ are obtained, matching or exceeding the global plasma parameters required for the Q = 10 ITER-FEAT operation [2]. Moreover, the plasma thermal stored energy content is approximately constant with increasing density (Fig.2, $\delta = 0.47$), as long as the discharge maintains Type I ELMs [3], up to $n_{ped}\sim n_{GR}$ (and $n\sim1.1n_{GR}$).

In the next sections it will be shown that with the highest triangularity, we observe an increase in the pedestal pressure with density, possibly due to marginal access to second stable region (ideal ballooning), as well as an improved core transport.

2. EDGE PEDESTAL, ELMS AND STABILITY.

This section analyses the results of gas/density scans carried out for *2.5MA/2.7T* and *2.0MA/2.7T* plasmas, $\delta\sim0.5$ and 15MW of NB additional heating. The discharges were fuelled with constant gas flow from the inner divertor, for improved efficiency [4]. Figure 3 shows the inner divertor D_α emission for 5 representative discharges of the *2.5MA* series. The usual relationship between Type I ELM frequency and density (f_{ELM} increasing with density) is 1not found for these high δ, high-density discharges. For $n_{ped}>70\%$ n_{GR}, the ELM frequency at first stops increasing and then, when nped is raised further by fuelling, f_{ELM} decreases to near the characteristic frequency of the unfuelled reference case (Fig.3). When the fuelling is increased further (Pulse No: 52739, Fig.3), a transition to Type III ELMs occurs.

The reduction of the ELM frequency with density is correlated with a characteristic increase of the D_α signal between ELMs. An example of such behaviour is shown in Fig.4. The high-density Pulse No: 52997 has reduced ELM frequency compared to the low gas reference case Pulse No: 52995. In between ELMs, we see the typical structure in the D_α, with a clear enhancement of the base-line emission.

In general, the pedestal pressure of Type I ELMy H-modes in JET is not constant for increasing density, and it scales approximately as $1/n^2$ [1]. In contrast, the reduction in f_{ELM} at high density corresponds to a change in the trend of the pedestal temperature, which stops decreasing with density. As a consequence, the pedestal pressure increases, although not back up to the low-density values

(Fig.5, comparing Pulse No: 52995 and Pulse No: 52999). This is associated with good energy confinement, with the plasma energy content remaining ~ constant with density, as shown in Fig.2.

The interpretation of this change in the pedestal parameters and in the ELM behavior is still under discussion. Inspection of the MHD frequency spectrum associated to the f_{ELM} anomaly, shows a broadband activity up to *50kHz* in between ELMs, unique and characteristic to these cases. The larger D_α spikes are identified as standard Type I ELMs. The appearance of the broadband MHD signal, the high pedestal density and the pedestal temperature just marginally above the critical value for the Type I-III transition [3], are reminiscent of the characteristic signature of Type II ELMs as reported by ASDEX-U [5], as well as of some features of the EDA mode in Alcator-C Mod [6], although q_{95} here is lower than in both experiments. Simple power balance considerations show that the change in the D_α behaviour is associated to an increased transport between ELMs, again similar to observations for Type II and EDA modes. The Type I ELMs prompt energy losses are reduced compared to ELMs of the same frequency but at lower n_e and higher T_e [7], consistently with an edge collisionality driven loss mechanism for ELMs. For the particular case of the 2.5MA series, the ELM contribution to the loss power goes from 7 to 3MW, at ~ constant P_{in}, $P_{rad,bulk}$ and W_{th}.

Modeling of the edge stability of these plasmas is in progress. The JETTO code plasma analysis coupled to the ideal ballooning code IDBALL [8] for the 2.5MA case shows access to ideal ballooning second stability, at least over part of the edge pedestal region (ψ *>0.97*). This result is qualitatively consistent with the observed increase of the pedestal pressure and the decrease of the Type I ELM frequency with density. Unfortunately, the measurement of the pressure gradients with the edge LIDAR [9] is limited by the space resolution of the system, thus precluding a direct comparison with the JETTO computed pedestal pressure profiles.

In fact, for the 2.5MA case with Type I ELMs, the measured pressure gradient ∇p_{ped} in the pedestal region is always at least *240 kPa/m*, and any change of the gradient with density is not resolved. This is not any more the case during the Type III ELMs phase, such as in Pulse No: 52739 after 19s (Fig.3). This transition corresponds to a reduction of the pressure gradient in the pedestal region down to ~180kPa/m, indicating indirectly that the edge pressure gradient sustained during the enhanced D_α phases is substantially higher than for Type III ELMs.

3. CORE PROFILES AND TRANSPORT.

The loss of pped with density is smaller at high δ compared to standard JET ELMy H-modes, in particular when the Type I ELM frequency starts to decrease at high nped,. Nonetheless, for increasing density, p_{ped} is somewhat reduced compared to the unfuelled reference case, and of course, the pedestal temperature reduced compared to reference. It follows that the experimental observation that the total stored energy is ~ constant with density implies that the core confinement of these discharges is constant up too the highest density. Therfore, in this section we analyse the changes in the core density and temperature profiles, for the *2.5MA/2.7T* series of discharges with δ ~0.5 and P_{in} = *1.5MW*.

The variation in density in the scan is quite large, from approximately *6* to *10 10^{19} m^{-3}* at the

pedestal. This implies that the central NB power and particle deposition profiles varied considerably (the central power density gradually decreases, down by ~2, and becomes very flat).

In first approximation, if the core temperature profiles were self-similar, the combination of constant W_{th} and off-axis heating should imply self-similarity in the density profiles or density peaking with density. The analysis of the n profiles shows that the characteristic timescale for the evolution of the density profile in the high δ discharges, at constant P_{in} and Φ_{GAS}, is of the order of *3s*, corresponding to *6-7 δ_E*.

In contrast, the pedestal density reaches quasi-steady state on a shorter time scale, typically ~1s. The density of most of these plasmas does not reach true steady state in the ~6s of additional heating although the "residual" time evolution is quite small and the peaking constant, hence the term quasi steady state used above. The final peaking factor npeak (defined as the ratio of the central to the pedestal line average density) decreases with n from pulse to pulse, as shown in the inset of Fig. 5 (for the analysis of spontaneous density peaking, see [10]). The current density profile is of course evolving in these discharges, but normal sawtooth activity is maintained in all pulses.

Ion and electron temperature are coupled in these discharges, due to the high density, and decrease for increasing density, from *~5keV T_i – 4keV T_e* at *80% n_{GR} to ~2.2keV* at *n~1.1n_{GR}*, but they exhibit different profile behaviour. We find that the ECE Te profiles are self-similar, at least up to *n~90%n_{GR}* (beyond that ECE emission is cut-off) whilst, as shown in Fig.5, the T_i profiles are not stiff, and they become more peaked as the density increases (each trace is Fig.5 is the average of 3 profiles taken at the end of the constant power phase of each discharge, plotted on the region outside the sawtooth inversion radius), consistently with the reduction in n_{peak} at ~constant Wth. Preliminary TRANSP analysis of these discharges indicates a reduction of χ_{eff} across the radius of the plasma for the discharges at the highest density. The interpretation of this unusual result is in progress, but the phenomenology of the high δ, high density discharges studied here seems to be different from what reported from other experiments. In particular, in [11], the good energy confinement of DIII-D gas fuelled ELMy H-modes at $n>n_{GR}$ is ascribed to the increased density peaking, with stiff T_e and T_i core profiles, in contrast with our finding. For a discussion of the role of input power, refer to [3].

4. PLASMA GEOMETRY EFFECTS.

The role of plasma shape in the pedestal and global confinement at high density has also been investigated by comparing plasmas with the same upper δ, but with different lower δ (Fig.6), at the same I_p, B_t and similar NB power (15 vs. 16.5MW). Although the geometry of the two configurations is different near the X-point (δ_L reduced from *0.4* to <u>0.3</u>), the variation in the average equilibrium properties near the edge is small, with the shear and q (at 95% of the flux) differing by *<10%*. Nonetheless, the configuration with higher δ_L (and higher <δ>) achieves higher confinement at higher density, as well as higher pedestal pressures.

The n_e-T_e diagram for the two gas/density scans (top of the pedestal values, constant P_{in}) is shown in Fig.8. The lower δ_L plasmas have, for a given n_{ped}, lower T_{ped}, and reduced pedestal pressure

across the density range. Moreover, the transition to lower confinement, Type III ELMs, occurs at lower density for the lower δ_L plasmas.

The "anomaly" in the Type I ELM frequency at high density, described in Section 2 is observed also at low δ_L, although this change in ELM behaviour for the low δ_L occurs very near the Type I-III transition, and is sustained in a much reduced nped window. The lower δ_L has a strong effect on both the Type I ELM frequency and prompt energy loss per ELM. In particular at high n_{ped} (n_{ped} ~90% n_{GR}, ~9×10^{19} m^{-3}), f_{ELM} for $\delta_L = 0.3$ is ~40Hz, to be compared to ~12Hz for $\delta_L = 0.45$. The respective ELM energy losses are *4-5%* and *8-9%* of W_{ped}.

ELM losses of about 4% are very close to the acceptable value for the ITER W divertor (3.6%), although in the experiment this is obtained at the cost of ~10-15% Wth reduction. This reduction in the total stored energy content and its trend with density (Fig.9) for the low δ_L plasmas are consistent with the reduced pedestal pressure.

CONCLUSIONS.

The positive effect of plasma shaping for achieving high density with high confinement in ELMy H-modes has been confirmed and extended in recent JET experiments. Plasma with δ and κ close to the ITER specifications have achieved n/n_{GR}, H and β_N required for the Q=10 ITER operation.

For n_{ped}>70 n_{GR}, the frequency of Type I ELMs decreases with density. Specific MHD broadband fluctuations and enhanced D_α are observed in the inter-ELM period. Similarities with Type II ELMs and EDA regimes are observed, although total Type I ELM suppression has not been achieved. 1-D stability calculations indicate a possible access to second stability.

For the same discharges, improved core confinement is observed at high density, with moderate density peaking and non-stiff core T_i profiles.

Finally, the reduction of δ near the X-point affects very little the poloidal averaged equilibrium parameters, but it nonetheless results in reduced Tped and more frequent, smaller Type I ELMs. The size of the ELM losses (~4-5%) approaches values acceptable for the W ITER divertor. 2-D MHD stability calculations such as those in [12] are probably required to model these geometry effects.

REFERENCES
[1]. G Saibene et al. Nuclear Fusion **39** (1999) 1133
[2]. ITER EDA Doc. Series **N19**, IAEA (2000), I.2.3
[3]. R Sartori et al., this Conference
[4]. C Maggi et al, 26 th EPS, ECA, **23J** (1999) 201
[5]. J Stober et al., to be published in Nuclear Fusion
[6]. A Hubbard et al, Phys of Plasmas **8** (2001) 2033

[7].   A Loarte et al., This Conference

[8].   V Parail et al., This Conference

[9].   M Beurskens et al., this Conference

[10].   M Valovic et al., this Conference

[11].   T Osborne et al., Phys of Plasmas **8** (2001) 2017
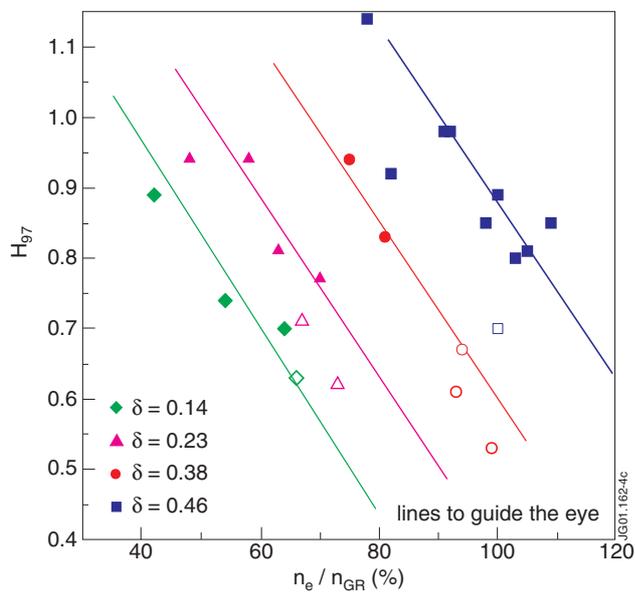
[12].   L.L Lao et al., Nuclear Fusion **41** (2001) 245

Figure 1: Confinement enhancement factor (H_{97}) as function of the Greenwald number n_e/n_{GR}. The new data for $\delta = 0.47$ are compared to triangularity scans from JET MkII experiments [1].
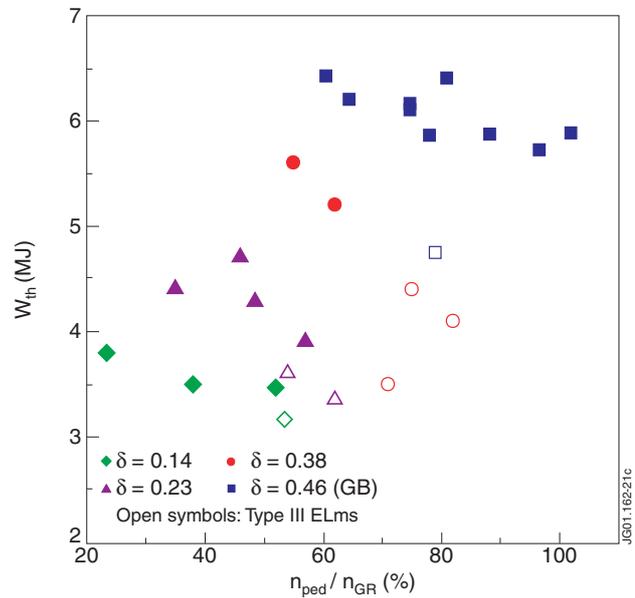

Figure 2: Thermal plasma stored energy W_{th} for the same discharges as in Figure 1 (2.5MA/2.7T), plotted against the normalised pedestal density n_{ped}/n_{GR}. Each point represents a different discharge.
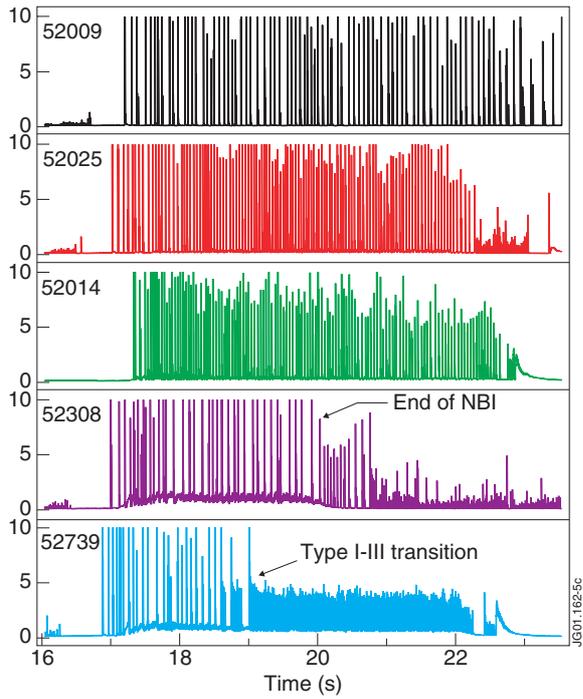
Figure 3: D_α emission from the inner divertor (a.u.) as function of time for a subset of discharges at 2.5MA/2.7T, $\delta \sim 0.5$, for increasing gas fuelling rates.
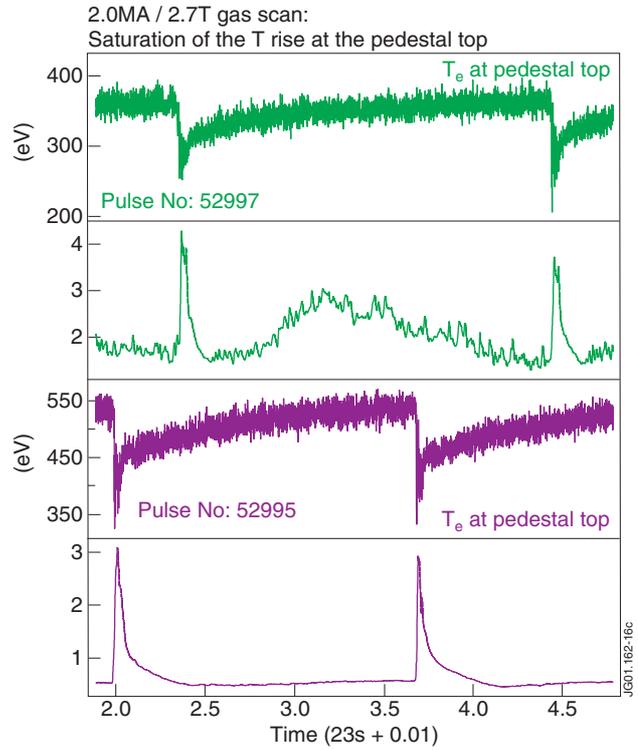

Figure 4: Time evolution of the T_e at the top of the pedestal and of the outer divertor D_α for two 2.0MA/2.7T ($q_{95}\sim3.8$), $\delta\sim0.5$ pulses: 52997 ($n_{ped}=72\%$ n_{GR}) and Pulse No: 52995 ($n_{ped}=48\%$ n_{GR}). Note the enhanced D_α levels in Pulse No: 52997.
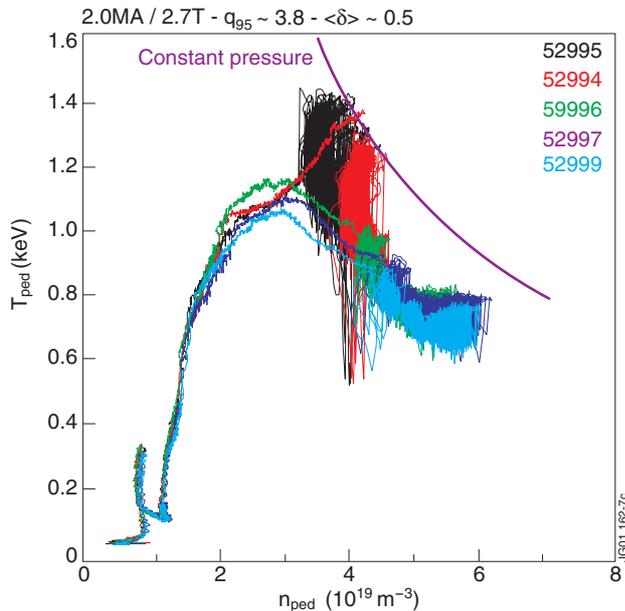

Figure 5: n_e-T_e diagram for a gas/density scan for 2.0MA/ 2.7T, $\delta \sim0.5$, 15MW P_{in}. Values at the top of the pedestal. All the discharges are in the Type I ELM regime.
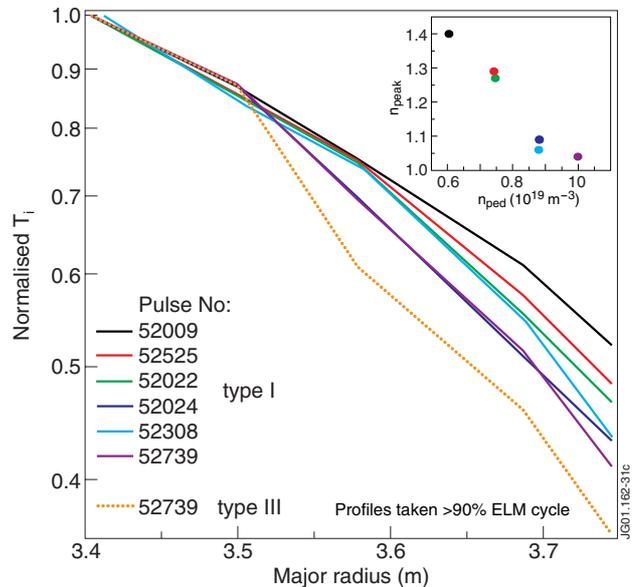

Figure 6: CX T_i profiles for a subset of the d ~0.5 discharges in Fig.1. Each trace is the average of 3 profiles, taken >90% into the ELM cycle, and normalised to its maximum. the inset shows, npeak versus n_{ped} for the same discharges and time slices
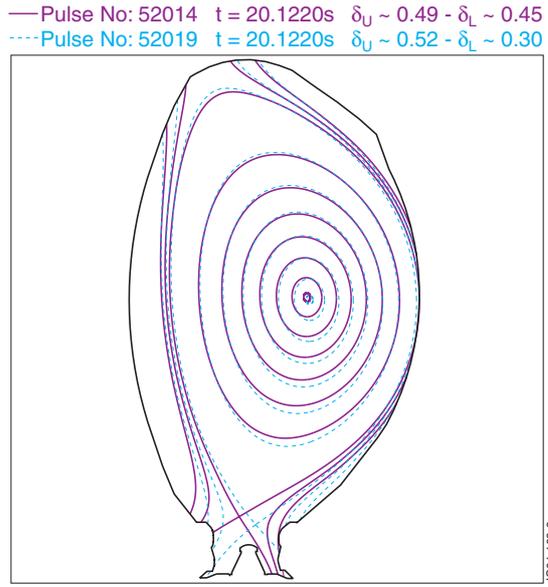
Figure 7: EFIT equilibrium reconstruction of the two configurations used to investigate the role of the lower δ
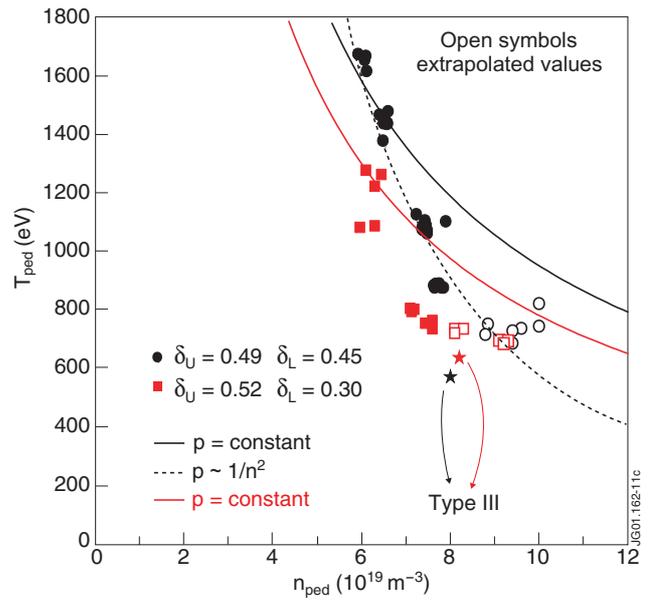

Figure 8: n_e-T_e diagram for gas/density scans for the two configurations. The open points are T_{ped} values at the beginning of the ELM cycle before the ECE cuts off.
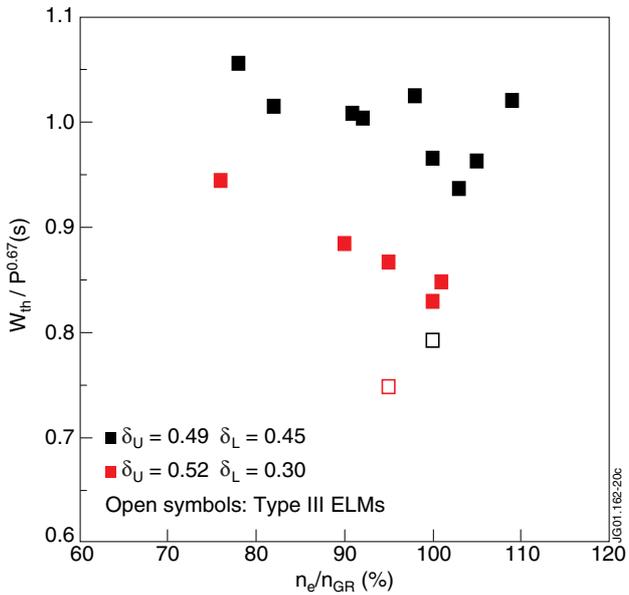

Figure 9: Comparison of W_{th} for the two configurations. W_{th} is normalised to account for the difference in P_{in} in the two series of density scans.